LOW SPEED STREAKS INSTABILITY OF TURBULENT BOUNDARY LAYER FLOWS WITH ADVERSE PRESSURE GRADIENT

J.-P. Laval
(1) CNRS, UMR 8107,
F-59650 Villeneuve d Ascq, France
(2) Univ Lille Nord de France,
F-59000 Lille, France
Jean-Philippe.Laval@univ-lille1.fr

M. Marquillie
(1) CNRS, UMR 8107,
F-59650 Villeneuve d Ascq, France
(2) Univ Lille Nord de France,
F-59000 Lille, France
Matthieu.Marquillie@univ-lille1.fr

U. Ehrenstein
Aix Marseille Univ, IRPHE UMR 6594,
CNRS, F-13384 Marseille 13, France
ehrenstein@irphe.univ-mrs.fr

ABSTRACT

A direct numerical simulation (DNS) of a turbulent channel flow with a lower curved wall is performed at Reynolds number $Re_\tau \simeq 600$ at inlet. Low-speed streak structures are extracted from the turbulent flow field and base flows formed with conditional streaks averages, superimposing the mean streamwise velocity profile, are used for linear stability analyzes. The instability in the presence of a strong pressure gradient at the lower wall is shown to be of varicose type, whereas at the upper wall (with weak pressure gradient) varicose and sinuous unstable modes can coexist. The onset of the dominant instability mechanism of varicose type is shown to coincide with the strong production peaks of turbulent kinetic energy near the maximum of pressure gradient on both the curved and the flat walls. The size and shape of the counter-rotating streamwise vortices associated with the instability modes are shown to be reminiscent of the coherent vortices emerging from the streak skeletons in the direct numerical simulation.

INTRODUCTION

The turbulent boundary layer flow subject to an adverse pressure gradient (APG) induced by curvature is of crucial importance for many applications including aerodynamics of airfoils, ground vehicles or turbine blades. Significant progress is needed in understanding the near wall turbulence in order to improve the theoretical and numerical models. The available numerical models usually fail to predict flows at the onset of separation as they are based on scaling which are no more valid with pressure gradient. In flows with adverse pressure gradients, a strong secondary peak of turbulent kinetic energy has been observed experimentally [1] and numerically [2] in many configurations with different intensity of pressure gradient [3] and is not yet fully explained. Therefore, a careful analysis of turbulent structure generation mechanisms is an opportunity to make progress in understanding the physics of such flows in order to improve statistical models for turbulence.

TURBULENCE STATISTICS

Using the numerical solution procedure documented in [4], a database of channel flow with curved wall has been generated at Reynolds number $Re_\tau \simeq 600$ at inlet. At this Reynolds number, the flow slightly separates at the lower curved wall and is at the onset of separation at the upper wall. Therefore, two different configurations of pressure gradient as well as the effect of wall curvature can be investigated and compared. The pressure coefficient at the two walls is reported in Fig. 1. The adverse pressure gradient region starts at $x = -0.2$ at the lower wall and is slightly shifted downstream ($x = +0.3$) at the upper wall.

As already been observed in most turbulent wall bounded flows with adverse pressure gradient, a second peak of turbulent kinetic energy appears and moves away from the wall. This second peak is present at the two walls but is more intense at the lower wall. The streamwise evolution of the corresponding peak of streamwise turbulent intensity is presented at the lower wall in Fig. 2. Owing to the non-homogeneity in the streamwise x-direction, in the following, two sets of wall units are considered. Local wall units are denoted conventionally with the superscript $+$ and reference wall units based on u_τ^o at the inlet have the superscript $\star$. The wall peak near $y^\star = 10$ at the bump summit $x = 0$ grows and moves away from the wall when progressing along the rear part of the bump. At approximately $x = 1.2$ a new near wall peak is

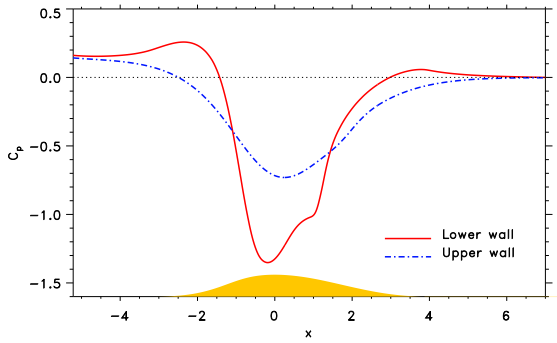

Figure 1. Pressure coefficient $C_p = (P - P_o)/\left(\frac{1}{2}\rho U_{max}^2\right)$ at the two walls

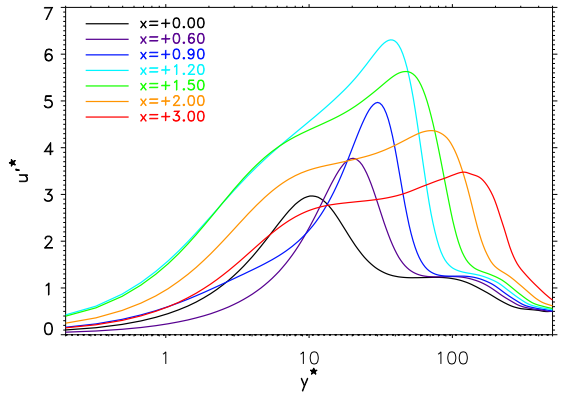

Figure 2. Normal profiles of the streamwise turbulence intensity at the lower wall

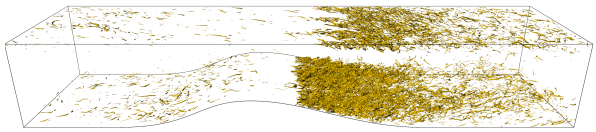

Figure 3. Visualization of intense vortices by iso-value of the Q–criterion for the whole simulation domain.

regenerated whereas the original one decreases and continues to move apart.

This peak of turbulent intensity corresponds to the generation of vortices much stronger than typical vortices in the buffer and log region of a boundary layer without pressure gradient. These intense vortices are visualized at the two walls in Fig. 3. At the lower wall they are generated within a short streamwise region near $x = 0.5$ slightly downstream the bump summit. Their spanwise distribution is also much more homogeneous at the lower wall than at the upper wall. The starting locations of these intense vortices coincide with the increase of the turbulent kinetic energy peak. The observed production of intense vortices in the APG regions is likely to be associated with some instability mechanism of coherent flow structures, such as streamwise velocity streaks which are known to be key features of wall turbulence.

Figure 4. Results of the detection of the low-speed streaks at the lower wall in the converging part of the domain. The skeletons are indicated with dark tubes down to $x = 1.3$ as the 3D visualization indicates that the streaks are totally destroyed further downstream.

STREAKS DETECTION

Evidence of wall-turbulence generation through the instability and breakdown of low-speed streaks has been provided in [5] for the zero-pressure gradient boundary-layer. The mechanism leading to breakdown is shown to be consistent with the regeneration cycle of wall turbulence [6]. Focusing on the role of streak instability dynamics in wall turbulence production, Schoppa and Hussain [7] consider a representative steady low-speed streak superimposed to a turbulent mean velocity profile, corresponding to minimal channel turbulence [8]. Streak instability in APG turbulent boundary layers has found less attention. Here, we aim at assessing a possible link between the above mentioned turbulent kinetic energy peak observed in our simulation data and a streak instability. For this purpose, an algorithm based on image processing technique is used to isolate from the turbulent database averaged low-speed streak structures.

The first step is to apply a thresholding on the streamwise velocity fluctuation used as a detection function. Then, topological corrections are applied to the 3D binary images before a *skeletonization* algorithm is used to extract the streaks center-lines. At this point, a *prunning* algorithm is applied to simplify the streaks structure by removing the smallest structures and the smallest branches of complex structures. This procedure is able to detect all significant individual low-speed streaks (called simply *streaks* in the following) of a near wall turbulent flow as can be seen in Fig. 4, low-speed streaks being shown in the vicinity of the bump. The objective of the present study is not to accurately characterize the full range of streaks but rather to define a realistic streak in average. For this purpose a conditional average of velocity fields in the normal-plane (y,z) in the vicinity of the detected streaks have been computed. An averaging window with fixed size has been centered at the spanwise location of each streak skeleton. In the case of multiple branches only those which are sufficiently long and representative of well-defined streaks were retained for the statistics.

Several statistics such as the intensity, the size and the position of detected streaks have been computed. These statistics provide evidence for the large distribution of each parame-

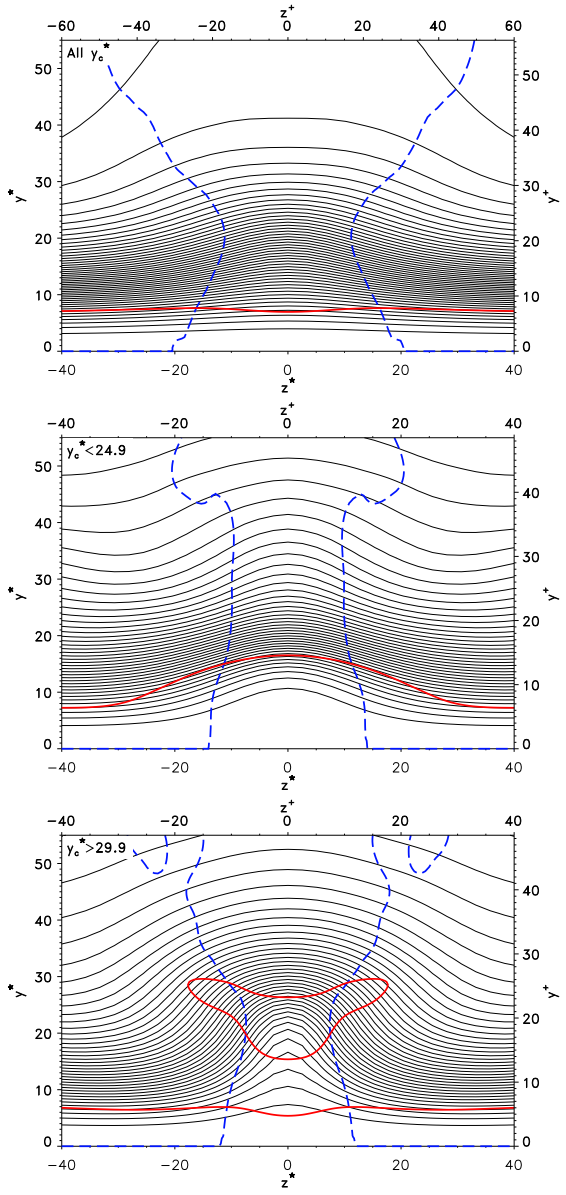

Figure 5. Contour plot of streak base flow for the conditional average using the distance of the streak's center $y_c^\star$ from the wall. **Upper plot:** all streaks, lower wall at $x = 0.22$. **Middle plot:** upper wall at $x = 1.29$, 20% lowest streaks. **Lower plot:** upper wall at $x = 1.29$, 20% highest streaks. The red continuous line and blue dash lines indicate the location of $\partial^2\bar{U}/\partial^2 y = 0$ and $\partial^2\bar{U}/\partial^2 z = 0$ respectively.

ters corresponding to the diversity of streaks. Therefore, in addition to a conditional average of streamwise velocity (called simply *streak base flow*) on all streaks at each streamwise location of the two walls, the same averaging procedure conditioned by the intensity of streaks or its distance from the wall has also been performed. The corresponding averaged streamwise velocity $\bar{U}$ is shown in Fig. 5 at one location for each wall which will be shown hereafter to be associated to instability. The location of normal and spanwise inflexion points have been superimposed on each graph. The normal inflexion

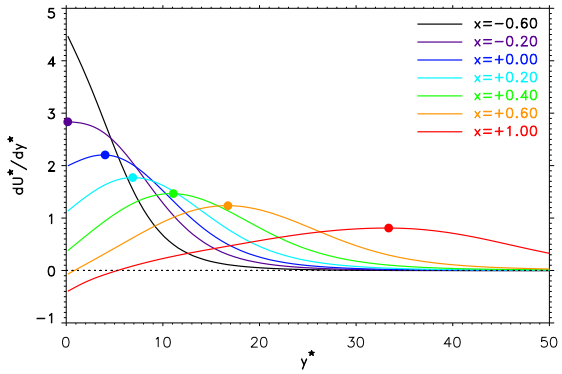

Figure 6. Profiles of the wall-normal derivative of the mean streamwise velocity at several streamwise positions at the lower wall. An inflexion point (indicated by a solid circle) is generated near $x = -0.2$ and moves away from the wall

points on the streak base flow at the lower wall are almost independent of the spanwise direction and located at less than 10 wall units at this streamwise location. This indicates that the presence of a streak only modifies slightly the normal inflexion points which are a feature of the mean streamwise velocity profile. The derivative of the mean streamwise velocity, see Fig. 6, at the lower wall shows that a normal inflexion point appears at $x = -0.20$ precisely at the change of sign of the pressure gradient (see fig. 1) since, from the averaged Navier Stokes equations, at the wall, we have $\nu\,\partial^2 U/\partial y^2 = dP/dx$. Then, the normal position of the inflexion points moves away from the wall as the peak of turbulent kinetic energy does. This connection between the inflexion point and the peak of turbulent kinetic energy has been noticed by George *et al* [9] for APG turbulent flows at higher Reynolds number.

The streak base flow is rather different at the upper wall as the inflexion line in this case is affected by the streak. The base flow computed with the 20% of streaks closest to the wall and the 20% highest are very different from the corresponding streak-averages at the lower wall. This is due to the lowest values of pressure gradient which leaves a stronger influence of the streaks in general and especially for the highest streaks.

STREAKS INSTABILITY

The streak base flow is considered as the basic state for a modal instability analysis. Owing to the non-parallel converging-diverging channel and the resulting pressure gradients, the averaged flow quantities depend on the streamwise coordinate. Consequently, a normal-mode analysis assuming homogeneity of the disturbance in the streamwise direction is strictly speaking not valid anymore. It would however be impossible to consider a full stability analysis for a base flow depending on the three space-coordinates. Indeed, already for the parallel flow assumption the stability operator is of very large size, the sharp gradients of the base flow near the wall necessitating a high resolution in (y,z). Consequently, the locally parallel flow hypothesis appears to be necessary

for the analysis to be feasible.

In this parallel setting, the velocity and pressure perturbations are

$$\mathbf{u}(x,y,z,t) = (\hat{u}(y,z),\hat{v}(y,z),\hat{w}(y,z))\, e^{i(\alpha x-\omega t)}, \quad (1)$$

$$p(x,y,z,t) = \hat{p}(y,z)\, e^{i(\alpha x-\omega t)}, \quad (2)$$

the perturbation being unstable if the imaginary part ω_i of the complex temporal eigenvalue $\omega = \omega_r + \omega_i$ is positive. Linearizing the Navier-Stokes at the base state $(\bar{U}(y,z),0,0)$, the perturbation modes are solution of the perturbation equations for $\hat{u},\hat{v},\hat{w}$. Details of the equations and of the numerical methods used for the 2D stability analysis can be found in [10] and [11]. According to the commonly used classification, varicose modes are such that the streamwise perturbation velocity component $\hat{u}(y,z)$ is symmetric, that is $\hat{u}(y,-z) = \hat{u}(y,z)$, whereas $\hat{u}(y,z)$ for sinuous modes is antisymmetric with $\hat{u}(y,-z) = -\hat{u}(y,z)$.

For the streak base flow near the lower wall, several streamwise locations in the region near $x = 0.2$ has been considered. The streamwise location $x = 0.22$ is seen to be very close to the margin of neutral instability whereas slightly downstream the base state is clearly unstable. It has to be emphasized that the observed onset of the instability at $x = 0.22$ is also the location where the turbulent kinetic energy starts to increase. The instability is associated with varicose modes only. Actually, at the lower wall and in the presence of strong pressure gradient there is some evidence that the mean velocity inflection point determines the streak instability strength, the averaged streak being however responsible for the mode shape.

For the streak base flow near the upper wall, the region downstream $x = 1.1$ has been considered. Considering the base flow with the average of all the streaks, the streak instability is maximum at $x \approx 1.33$ but is weaker than at the lower wall. However, as noticed from the streak base flow (fig. 5), the distance of the streak center from the wall seems an important parameter as it completely modifies the shape of the inflexion lines contrary to the streak base flow at the lower wall. It is therefore likely that the mean velocity profile at the upper wall only plays a minor role for the instability. Considering the different conditional averages at $x = 1.29$ based on the streaks distance from the wall, sinuous modes are found to be unstable for the highest streaks, whereas varicose modes similar to the ones observed at lower wall are the most unstable for the streaks closest to the wall.

At the lower wall, the shape and size of unstable varicose modes ($\simeq 150^\star$ width and $\simeq 200^\star$ length) compare surprisingly well with the hairpin-type structures extracted from the DNS slightly downstream the location of streaks instability. Example of these structures are shown in Fig. 7 using the Q-criterion in the instability region at the lower wall. A characteristic hairpin-type structure is presented (upper plot). A streak is present in front of the structure, a portion of which being visualized with its skeleton. These structures are representative of the vortices generation mechanism as it can be seen from the lower plot where several hairpin-type of structures can be identified within the spanwise direction at a given time.

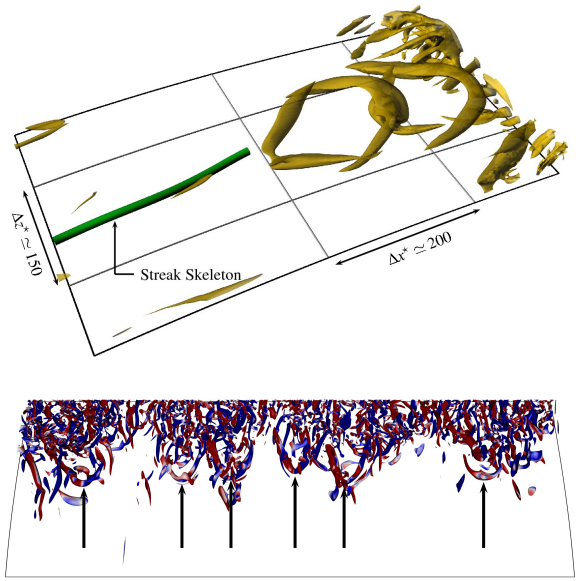

Figure 7. Visualization of a well defined coherent structures at the lower wall in the region of instability. **Upper plot**: isovalue of the Q-criterion. A streak is present in front of the structures, a portion of which being visualized with its skeleton. **Lower plot**: coherent structure events along the spanwise direction for $0.4 \leq x \leq 1.41$ (the arrows point at hairpin-type vortices visualized by Q-iso-surfaces, colored with the streamwise vorticity).

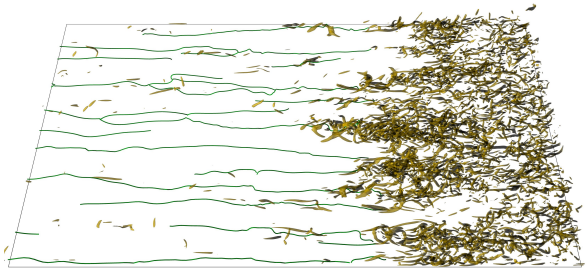

Figure 8. Visualization using Q-criterion of intense vortices (yellow) and low speed streaks skeleton (in green) at the upper wall in the region of instability

The situation is more complex at the upper wall as both sinuous and varicose modes may coexist and the streamwise region of possible streaks instability, depending on the streaks characteristics, is longer than for the lower wall. The instability results at the upper wall is in agreement with the observation of the turbulent vortices in the DNS. As the instability is essentially due to the streaks,x the vortices are strongly linked to the location of the incoming streaks as can be observed in Fig. 8. As a consequence, the spanwise distribution of intense vortices is much less homogeneous and leads to a second peak of turbulent kinetic energy weaker in intensity than at the lower wall. However, this peak is still significantly larger than the typical value for zero pressure gradient flow.

CONCLUSION

A direct numerical simulation (DNS) of a turbulent channel flow with a lower curved wall has been performed and a second peak of turbulent kinetic energy was observed at the two walls. In order to investigate the origin of the sudden production of turbulent kinetic energy, a streaks instability was conducted in the region of change of sign of pressure gradient. Considering the total average of the streaks which have been detected, the streak base flows proved to become unstable at some streamwise locations with respect to varicose modes. For conditional averages for the streak base flow, using the distance of the streak's center from the wall as a criterion, at the upper wall sinuous modes proved to become unstable too. At both walls the averages of streaks the closest to the wall exhibit the highest amplification rates for varicose modes. The corresponding three-dimensional perturbation structures are seen to be reminiscent of the hairpin-type vortex structures detected in the simulation as both the streamwise location and the size of the structures are in accordance. There is hence strong evidence that in the present APG wall turbulence the averaged streak instability dynamics is related to the local onset of strong production of kinetic energy. One may conjecture, whether the reported results are generic for adverse-pressure wall turbulence. Note that characteristic turbulent energy peaks seem to be a general feature in the presence of APG ([3]). To connect this behavior to streak breakdown will certainly to be interpreted in the light of turbulence modeling. Indeed, the mean turbulent velocity gradients are at the heart of Reynolds-averaged Navier-Stokes modeling, which is unlikely to be reliable in the presence of turbulence production peaks as a result of a streak instability mechanism.

REFERENCES

[1] M. Materny, A. Drozdz, S. Drobniak, and W. Elsner, "Experimental analysis of a turbulent boundary layer under the influence of apg.," *Achives of Mechanics*, vol. 60, pp. 1–18, 2008.

[2] J.-H. Lee and H. J. Sung, "Effects of an adverse pressure gradient on a turbulent boundary layer," *Int. J. Heat Fluid Flow*, vol. 29, pp. 568–578, 2008.

[3] S. I. Shah, M. Stanislas, and J.-P. Laval, "A specific behavior of adverse pressure gradient near wall flows," in *Progress in wall turbulence : understanding and modelling* (M. Stanislas, J. Jimenez, and I. Marusic, eds.), ERCOFTAC Series vol 14, (Villeneuve d'Ascq, France, April 21-23), pp. 257–265, Springer, 2010.

[4] M. Marquillie, J.-P. Laval, and R. Dolganov, "Direct numerical simulation of separated channel flows with a smooth profile," *J. Turbulence*, vol. 9, no. 1, pp. 1–23, 2008.

[5] M. Asai, Y. Konishi, Y. Oizumi, and M. Nishika, "Growth and breakdown of low-speed streaks leading to wall turbulence," *J. Fluid Mech.*, vol. 586, pp. 371–396, 2007.

[6] J. Jiménez and A. Pinelli, "The autonomous cycle of near wall turbulence.," *J. Fluid Mech.*, vol. 389, pp. 335–359, 1999.

[7] W. Schoppa and F. Hussain, "Coherent structure generation in near wall turbulence," *J. Fluid. Mech.*, vol. 453, pp. 57–108, 2002.

[8] J. Jiménez and P. Moin, "The minimal flow unit in near wall turbulence.," *J. Fluid Mech.*, vol. 225, pp. 221–240, 1991.

[9] W. K. George, M. Stanislas, and J.-P. Laval, "New insights into adverse pressure gradient boundary layers,," in *Bulletin of the American Physical Society, 63th Annual Meeting of the APS Division of Fluid Dynamics, Long Beach, California APS Bull, USA*, vol. 55 (16), 2010.

[10] M. Marquillie, U. Ehrenstein, and J.-P. Laval, "Instability of streaks in wall turbulence with adverse pressure gradient," *submitted to J. Fluid Mechanics*, 2010.

[11] U. Ehrenstein and F. Gallaire, "On two-dimensional temporal modes in spatially evolving open flows: the flat-plate boundary layer," *J. Fluid Mech.*, vol. 536, pp. 209–218, 2005.